

Hand Range Interface: Information Always at Hand With A Body-centric Mid-air Input Surface

Xuhai Xu
Tsinghua University
Beijing, China
xxh14@mails.tsinghua.edu.cn

Alexandru Dancu
Singapore University of
Technology and Design
Singapore, Singapore
alex@ahlab.org

Pattie Maes
MIT Media Lab
Cambridge, United States
pattie@media.mit.edu

Suranga Nanayakkara
The University of Auckland
Auckland, New Zealand
suranga@ahlab.org

ABSTRACT

Most interfaces of our interactive devices such as phones and laptops are flat and are built as external devices in our environment, disconnected from our bodies. Therefore, we need to carry them with us in our pocket or in a bag and accommodate our bodies to their design by sitting at a desk or holding the device in our hand. We propose *Hand Range Interface*, an input surface that is always at our fingertips. This body-centric interface is a semi-sphere attached to a user's wrist, with a radius the same as the distance from the wrist to the index finger. We prototyped the concept in virtual reality and conducted a user study with a pointing task. The input surface can be designed as rotating with the wrist or fixed relative to the wrist. We evaluated and compared participants' subjective physical comfort level, pointing speed and pointing accuracy on the interface that was divided into 64 regions. We found that the interface whose orientation was fixed had a much better performance, with 41.2% higher average comfort score, 40.6% shorter average pointing time and 34.5% lower average error. Our results revealed interesting insights on user performance and preference of different regions on the interface. We concluded with a set of guidelines for future designers and developers on how to develop this type of new body-centric input surface.

Author Keywords

Body-centric interaction; Mid-air input surface; Interface evaluation

ACM Classification Keywords

H.5.m. Information Interfaces and Presentation (e.g. HCI): Miscellaneous

Permission to make digital or hard copies of all or part of this work for personal or classroom use is granted without fee provided that copies are not made or distributed for profit or commercial advantage and that copies bear this notice and the full citation on the first page. Copyrights for components of this work owned by others than ACM must be honored. Abstracting witheredit is permitted. To copy otherwise, or republish, to post on servers or to redistribute to lists, requires prior specific permission and/or a fee. Request permissions from Permissions@acm.org.
MobileHCI '18, September 3 - 6, 2018, Barcelona, Spain
©2018 Association for Computing Machinery.
ACM ISBN 978-1-4503-5898-9/18/09\$15.00
<https://doi.org/10.1145/3229434.3229449>

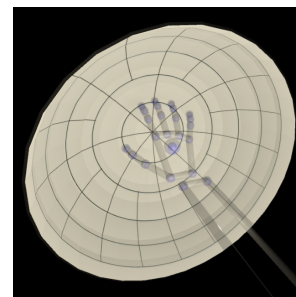


Figure 1: Interface in Virtual Reality

INTRODUCTION

Wearable technologies are game-changing: standalone LTE smartwatches [22, 34] have a potential to replace smartphones [2, 16], while head-worn displays could replace the LCD screens of PCs as the preferred workplace computer [29]. However, the interfaces of these wearable devices need to be improved in order to create efficient and flexible computing environments. For instance, smartwatch interfaces are mainly designed to support micro-interactions: short bursts of interactions, such as answering calls and receiving notifications [9]. These interactions mainly rely on a small 2D area on the wrist, together with just a few extra gestures [12, 41]. The gestures offer a limited expression of a user and limited control of the interface. In order to move beyond these micro-interactions and develop productive computing environments, additional interaction techniques are needed.

Body-centric interaction with mobile devices [7] and multi-surface environments [36] is a class of input techniques that allow a user to navigate and manipulate digital content in the space on and around the body. Wearable mid-air display [8] is a body-centric visual interface that presents information relative to the body, allowing a user to determine the distance of the visual content and to interact with it. These mid-air displays are “floating images in free space” [17, 32], always rendered relative to a part of the body.

Body-centric interfaces yield new opportunities for mobile human-computer interaction yet not fully explored. We pro-

pose a body-centric mid-air input surface that is *in reach*, *fast* and *comfortable*. This interface is always *in reach* because it is designed to be a virtual semi-sphere attached to a user's wrist and have a radius the same as the distance from the wrist to the index fingertip. A user can interact with the interface using their index finger on any position in 3D space since it moves as the user is moving their hand. The information is always available and can be accessed *fast* and *comfortable*. We envision this interface can be used to facilitate interaction in virtual reality (VR), augmented reality (AR) and even daily life when visualization techniques such as holographic projections are becoming commercial. Figure 1 shows our implementation of this semi-spherical interface in VR.

Pointing to a target on the mid-air interface means pointing to a 3D point on the semi-sphere. The curved surface of the semi-sphere can at all times be rotating together with the wrist or be fixed relative to the wrist (see Figure 3). Thus the pointing, target selection, and the user experience are different in these two conditions.

In order to evaluate the physical comfort, pointing speed and pointing accuracy when users operate with such an interface, we executed a user study with a pointing task to measure the interface's usability. We also compared the two movement strategies of the interface. The contributions of this paper are:

- A body-centric interface that is always within reach by being attached to the wrist of a user
- Insights from the evaluation of the two conditions comparing the interface's movement strategies relative to the wrist
- A set of guidelines to inform designers on how to develop this type of new body-centric interface

RELATED WORK

The background for our work comes from the areas of body-centric interaction, mobile projection, wearable on-body projection, mid-air gestures, and hand ergonomics. We review these areas in detail.

Body-centric Interaction

Chen et al. [7] proposed Body-Centric Interaction with mobile devices, a class of input techniques that allow a person to position and orient the mobile device to navigate and manipulate digital content anchored in the space on and around the body. These input techniques extend interactions beyond the small screen and are driven by a person's movement of the device on and around the body. BodyScape [36] proposed a body-centric design space for multi-surface interaction by evaluating two free-hand techniques, on-body touch, and mid-air pointing. The performance evaluation of body parts divided in 3 groups (dominant upper arm, dominant upper body, and lower body) found that upper body targets were faster for touching (1.4s) than lower limbs (1.6s). The input techniques in body-centric interaction can be applied in wearable computing through head-worn interfaces or futuristic mid-air interfaces. To the best of our knowledge, prior work did not investigate any mid-air "hand-centric" interface. Our work is the first one to employ the wrist as the center of a mid-air interface.

Virtual Windows around The Body

Wearable mid-air displays [8] present information relative to the body, allowing the user to determine the distance of the visual content and to interact with it. Ens et al. [10] aimed to develop "natural-feeling interactions" by improving mobile multitasking on virtual windows in head-worn displays with direct input. These virtual windows were situated in the empty space around the user and were compared against two baseline interfaces for switching between everyday mobile applications. They claim that this approach provides a 40% improvement in application switching time, highlighting the deficiencies of current view-fixed displays. As a follow-up [9], the authors developed input techniques for head-worn displays using hand tracking with a head-mounted depth camera and a small ring device. They explored a variety of input techniques to support high-precision, low-fatigue interaction techniques. In the two works of Ens et al. [9, 10], virtual windows are rendered relative to a user's body. However, in our work, we propose having the content attached to a user's hand at all time, which can reduce the fatigue of mid-air interaction and access time.

Wearable Displays Projected on Environment

Wear-Ur-World is a wearable gestural information interface using a head-worn projector and arbitrary surfaces [27]. Interaction techniques have also been prototyped with simulated wrist-worn projectors and wall surfaces [3]. Ota et al. [30] explored 16 body locations for wearing multiple projectors for navigation and a photo-slide show while walking and standing, displaying information on floors. The Ambient Mobile Pervasive Display [40] is a shoulder-mounted projector able to display on surfaces around the environment, the floor and the hand. Cauchard et al. [5] identified challenges of hand-held pico-projectors used on walls, desks, and floors, suggesting that this setting is unsuitable for many tasks. Motion-Beam [39] is a mobile projector that couples the movement of the projection to the imagery. ProjectorKit provides technical support for rapid prototyping of mobile projector interaction techniques [37].

Wearable Displays Projected on Body

Interaction with on-body projected interfaces has emerged after PALMbit [42] and Skinput [15] led the way towards this new research direction. Projection technology was used to investigate multi-touch interaction on the body and on arbitrary surfaces [13, 14, 15, 26]. Muller et al. [28] proposed employing flexion and extension to extend the input space of projective user interfaces. The user is able to browse a multi-layer information space by moving the hand towards or away from the body.

The communication with these interfaces happens in the air, employing the space around users to facilitate natural interaction. However, the 3D interactive space near the hand is still underexplored. In our work, we propose a new type of interface and measure users' performance and physical comfort of this interface.

Body Mapping and Gestures

Appropriating the human body as an input device is appealing not only because we have roughly two square meters of

external surface area, but also because much of it is easily accessible by our hands. Several approaches have been explored for on-body interaction, such as skin sensing technology using EMG [25], acoustic [15] or waveguide [44], and wearable tattoo based on gold leaf [19] or electronic skin [1].

Mapping the Body

Mapping body locations for input was explored in DigitSpace [18], a thumb-to-fingers interface, showing that people can discriminate 16 tap regions on their fingers. Gesture elicitation studies for single-hand microgestures [6] showed that when comparing with other gestures, taps are preferred by users because of their ease of use and conceptual simplicity. Weigel et al. [38] studied what type of gestures could be performed on-skin and what are the preferred input body locations for the purpose of on-skin input. Their experiment did not use any sensing technology, but involved only touching the bare skin on the upper limb with the fingers while the participant was seated at a desk. They found out that the forearm and the hand were the preferred body locations for on-skin input. These works argue that this on-skin input would be used for interaction with smartwatches and head-mounted displays, but none propose a visual display at fingers' reach. DigitSpace [18] illustrates text input, but displays on a smartwatch.

Single-hand micro-gestures

Single-hand micro-gestures (SHMGs) [6] are gestures performed by one hand on the same hand; they are subtle, can be performed anytime and anywhere, and can be performed naturally in public contexts. Out of the 16 consensus gestures in their elicitation study of SHMGs [6], 12 of them have been performed using the thumb as the main finger involved in the gesture. DigitSpace [18] provides a map of comfort regions of all fingers for tap and stroke paths of letters. The results showed that for the stroke paths, the highest comfort ratings were obtained for the index and middle finger of the dominant hand [18]. More recently, aiming to solve issues with the small screens of smartwatches: having to use two hands and the "fat finger" problem, Sun et al. [35] proposed a wrist-to-finger input approach that enables one-handed and touch-free target selection on smartwatches by tilting the wrist to point and using in-air finger tap to click. Rahman et. al [31] explored wrist-based interactions using a phone, investigating factors influencing tilt control. The experiment studied the three axes of wrist movement and found out that for flexion/extension and pronation/supination users are able to control 12 and 16 tilt levels respectively. These works explore comfortable gestures, but consider for interaction only displays of smartwatches and phones. Using the hand as the input surface center is a novel approach that can benefit gesture input and on-skin input research.

Ergonomics of On-hand Interface

Research in ergonomics has investigated subjective joint discomfort extensively. Yang et al. [43] and Marler et al. [24] found that participants felt comfortable the near neutral area but the discomfort increases significantly when joints approach their upper or lower limits. Khan et al. [20, 21] investigated the effect of wrist deviation, wrist flexion/extension

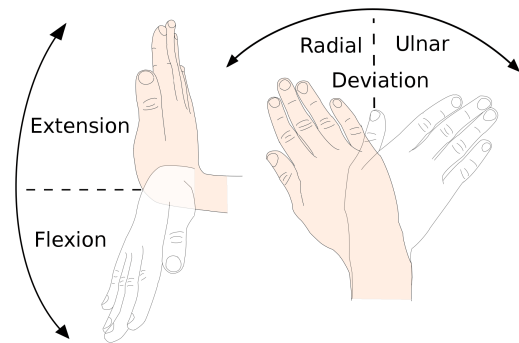


Figure 2: Hand motions: Left) Flexion and extension. Right) Ulnar and radial deviation.

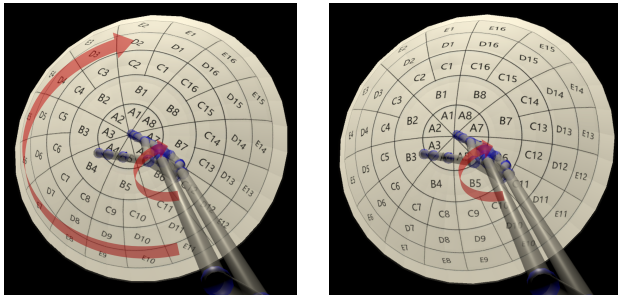
and forearm rotation on discomfort score (see Figure 2 for the postures). They found significant effects on the three main factors but no significance on any interaction factors. Li and his colleagues [23] looked into the joint motion of wrist deviation and flexion/extension. They found asymmetric convex hull of the wrist range of motion (ROM) when asking participants to perform extreme circumduction motions (max ulnar angle > max radial angle, max extension angle > max flexion angle). Carey et al. [4] found asymmetric contours about the discomfort level on the wrist's 2D motion maps (at the same percentage of ROM, ulnar discomfort < radial discomfort, extension discomfort < flexion discomfort). Huang et al. [18] looked into the hand anatomy restriction and the comfort zone of thumb-to-fingers interface. Participants were required to use their thumb to tap or draw shapes at specified finger segments and then rate comfort. They found that the comfort zone is mainly at the top two segments of the index and middle fingers. These works research the range of motion of the hand, but none have systematically studied the areas at hand range for the pointing task.

THE DESIGN OF THE INTERFACE

We propose a body-centric mid-air interface that is *in reach*, *fast* and *comfortable*.

- *In reach*: the interface needs to be convenient so that users can interact with it anywhere and anytime when needed. Hence the interface should dynamically follow users body to ensure an easy interaction.
- *Fast*: to have a smooth interaction, the elements on the interface should be able to be reached quickly. The interface is always relative to the finger position, which minimizes the time to access the information.
- *Comfortable*: the elements on the interface need to be easily accessible, and the interaction should be effortless. For instance, a button on the interface should be easy to reach. The interface needs to provide comfortable interaction.

We illustrated the design of the body-centric interface in VR (with HTC VIVE). The surface is set as a semi-sphere, and the center of the sphere is the imaginary center point of user's middle carpal. The design decision of a semi-spherical symmetric display is based on the natural hand range boundary that is almost a semi-sphere, as well as on a recent study



(a) Rotate with the wrist: Both the position and the orientation of the surface are bound to the wrist. The display rotates as the wrist rotates.

(b) Not rotate with the wrist: Only the position of the surface is bound to the wrist. The orientation is in line with the direction from the elbow to the wrist.

Figure 3: Two Designs of The Interface’s Movement. The arrows indicate the rotation of the hand and interface. The characters and numbers are used to show the orientation and identify of each region, as discussed in the next section.

showing that visualizing content on a circular display shape is considered more visually pleasing than a rectangular display [33].

Figure 1 presents the implementation under both scenarios.

The semi-sphere can be rotating with the wrist or be fixed relative to the wrist. We propose two designs of the translation and rotation of the interface.

- *Rotate with the wrist:* Both the position and the orientation of the interface is bound to the user’s wrist (middle carpal). So that it moves with the user’s hand and rotates as the user rotate their wrist (Figure 3a). It can be viewed as an additional part of the human body.
- *Not rotate with the wrist:* Only the interface’s position is bound to the user’s wrist. It follows the user’s hand but does not rotate with the wrist. The direction of the semi-sphere (from the center to the pole) is in line with the axial direction of users’ forearm. In order words, taking the direction from the sphere’s center to the pole as the y axis, the interface’s *roll* is fixed. Figure 3b shows this design.

We conducted a user study in virtual reality to evaluate and compare these two strategies concerning the physical comfort, as well as the speed and accuracy during pointing with the index finger.

USER STUDY

Participant

24 right-handed participants (12 Female) were recruited from the local university, averagely aged 27.7 (SD = 8.1). All participants claimed to have no previous injury on the right hand.

Apparatus

We used HTC VIVE with Unity 5.6.0 for showing a spherical surface at hand range.

Considering the cost for commercialized wearable systems for hand tracking in the near future, we employed Leapmotion sensor instead of expensive systems such as Optitrack to

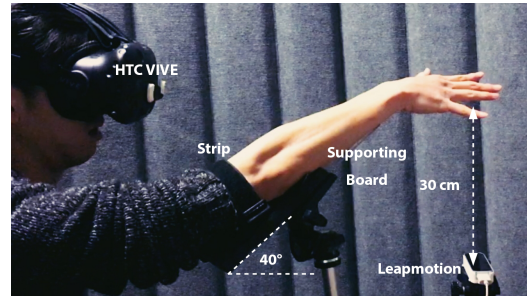


Figure 4: Experiment Setup

simulate a user experience that was more close to a futuristic affordable system. The experiment was held in a dark room with minimum visible light to avoid optical noise. We compared the Leapmotion with the Optitrack system at the 64 target points on the interface designed for the pointing task (as described in the next section) in both rotating and not rotating settings. The average tracking error of one author’s index fingertip with all his reachable regions was 4.43 mm (SD = 3.08). The average tracking latency was 32.9 ms (SD = 2.1).

We fixed the relative position of the Leapmotion and the VR tracking system in the physical space. Then, the Leapmotion was calibrated with the VIVE system by modifying the Leapmotion’s position in Unity, so that the hand’s relative position to a user’s head in the virtual space was the same as that in the physical space. Participants could see a simplified model of their hand and move it as if they were in the real world.

Participants were seated throughout the experiment. They were required to position their right arm on an adjustable plastic board and stretch the hand through a bracelet around the arm. The purpose of the bracelet was to keep their arm on the board. The bracelet was loose enough so that it did not limit any movement of the hand and arm. The board was placed on a tripod, and its height was adjusted to participants shoulder height. The angle of the board was 40° to make sure that participants could see the whole input surface without any occlusion. The Leapmotion was placed on another tripod and put beneath participants’ hand at approximately 30 cm. Figure 4 shows the setup of the experiment. Compared to the typical usage of the Leapmotion, i.e., mounted on the VIVE headset, we found in the pilot study that Leapmotion could track the hand more robustly when positioned under the hand.

Experiment Design

We used a within-subject, single factor design (whether the interface rotates with the wrist). All participants went through two sessions, i.e., the interface rotating with the wrist (namely *rotation* session) vs. the interface not rotating with the wrist (namely *no-rotation* session). The order of two sessions was counterbalanced. Throughout the experiment, only the index fingertip’s position was recorded.

Based on a two-people pilot study, we divided the semi-sphere into 64 regions (see Figure 3) to keep a balance between the simplicity of the experiment and a fine-grained evaluation of physical comfort, pointing speed and pointing

accuracy. We first split the surface into five circles in the latitude direction, each accounted for 18° . We named from interior circles to exterior circles as *A-E*. For the first and second smaller circles, we divided each of them into eight pieces in the longitude direction, with each pieces taking up 45° . The regions were numbered from 1 to 8 in the counter-clockwise direction, starting at the twelve o'clock direction. For the rest of 3 bigger circles, in order to maintain the similar area within all regions, we divided them into 16 pieces, with each taking up 22.5° . The regions were numbered from 1 to 16 in the counter clockwise direction, starting from the 12 o'clock direction. Figure 3 shows the characters corresponding to each region. The experiment was based on these 64 regions (8+8+16+16+16).

Calibration

The size of the body-centric interface needs to fit each participant's hand size. Hence at the beginning of each session, participants were asked to stretch their palm in the horizontal plane and stay static for 5 seconds. The distance between the index fingertip and the wrist center was obtained by Leapmotion. The surface was then scaled to the radius the same as the distance accordingly.

Task

The tasks in two sessions were set identical. Participants were asked to point to small red balls with a radius of one centimeter that appeared on the interface as fast and as accurately as they could, and maintain at the target position for 2 seconds. Touching the volume of the target ball would change its color from red to green. Sometimes participants' pointing was intermittent. Hence the point timing was set as cumulative.

The target sphere positions were placed at the center of each region in random sequence. If a target sphere was not reached, the participant could either ask the experimenter to skip it, or the next target would appear after 10 seconds. Figure 5 shows the snapshots during the pointing tasks. Between two target spheres of the 64 locations, a target sphere at the pole (azimuth) of the semi-sphere was introduced which brought the user's index finger to a neutral initial position, so that completion time could be correctly measured for each region.

For each of the 64 targets, both time and error were recorded. The pointing time was the elapse between the moment when the ball appeared and the moment when the participant's index fingertip first reached the small sphere's volume. If the ball cannot be reached, the time was marked as infinity.

The pointing error was the average distance between the index fingertip and the ball center. The record of the distance started once the participant first reached the ball and ended once the pointing time reached 2 seconds. The distance was calculated at a frequency of 30 Hz. Note that the timing is cumulative.

Physical Comfort Evaluation

After the pointing task, participants were asked to rate the physical comfort of the 64 regions in a 5-point Likert Scale (1: very uncomfortable - 5: very comfortable). If there were

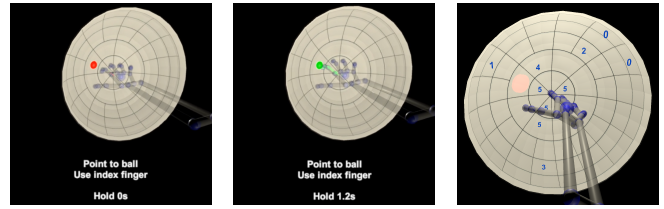


Figure 5: Left & Middle) Snapshots during Pointing Task. The color of the ball will change from red to green when the index fingertip reaches the ball. Right) Snapshots during Rating. Each region is rated on a 5-point Likert Scale (1: very uncomfortable - 5: very comfortable). If some region is not reachable, it is marked as 0. The red light indicates the next region for rating.

more than one posture to reach a region, participants were required to report the score of the most comfortable posture. If a region was not reachable, it was marked as 0. Each participants' data was standardized by the min-max procedure [11].

The regions were lit up one by one in random order. For each region, participants were required to reach it from the surface center to experience the whole pointing procedure. The right part of Figure 5 indicates the rating process.

Procedure

Participants were first asked to complete a demographics questionnaire. Then, the experimenter introduced the purpose of the experiment. Before performing tasks with the first session, participants put on the VIVE headset and place their right hand on the plastic board and in the strip.

All participants began with a test trial to practice the calibration stage and the pointing task. After they claimed that they understood the procedure, they started the *rotation* or *no-rotation* session. The two conditions were balanced over the number of participants. Participants had a 3 minutes break before entering the next session. Finally, they were required to finish a simple questionnaire with two questions asking which interface type they preferred and their additional comments.

Each session required participants to point at and evaluate 64 positions, which generated 64 data points for time, error and physical comfort respectively. Overall, the experiment contained 3072 trials (64 regions \times 2 sessions \times 24 participants). It took each participant approximately forty minutes to finish the study.

RESULTS

Within each session, the physical comfort, pointing time and pointing error shared similar patterns. The pointing task contained targets that were not reachable because the semi-sphere was larger than the range of the hand. One outcome of this study is the identification of the reachable regions on the semi-sphere. Figure 6 and Figure 7 show 3d-visualization as heat maps of the 64 regions' raw data on the three metrics (comfort, error, completion time, as well as not reachable areas in Figure 6). Figure 9 and Figure 10 present the heat maps after smoothing for a better visualization. Some regions' time and error marked as infinity (not reachable). These values were replaced for data analysis by $(\max(\text{time}_{\text{reachable}})+3*\text{std}(\text{time}_{\text{reachable}}))$ and

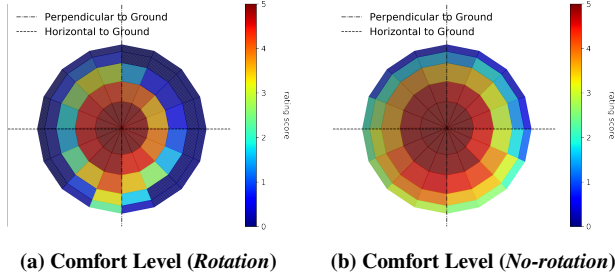


Figure 6: Unsmoothed Heat Map of Average Physical Comfort Score in Two Sessions. The regions with grid indicated that none of the 24 participants could reach them during the rating task. There are 17 such regions in the *rotation* session while zero region in the *no-rotation* session.

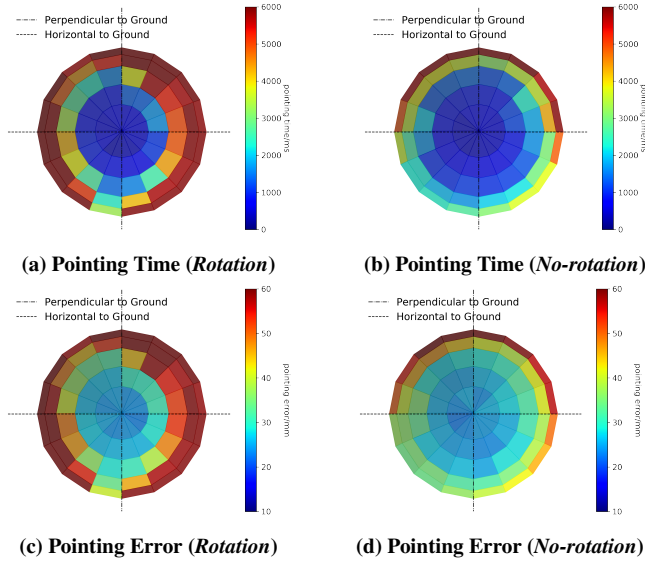


Figure 7: Unsmoothed Heat Map of Average Pointing Time And Error in Two Sessions. Note that the patterns are reversed against Figure 6 because time and error are “smaller is better” while physical comfort score is “larger is better”.

$(\max(\text{error}_{\text{reachable}}) + 3 * \text{std}(\text{error}_{\text{reachable}}))$ respectively. For physical comfort rating, the unreachable regions were coded as 0. Hence the rating scores had six levels (0 to 5). In the rest of this section, we first analyze each session’s results individually. Then we will compare the two designs.

Rotation Session

In this session, the interface was relatively static against participants’ hand. Hence it essentially reflected human hand’s fundamental properties.

Interior Circle Has a Better Performance Than Exterior Circle
We found that the regions closer to the interface’s center have a better performance, including higher physical comfort score, shorter time and lower error.

We first divided and merged each participant’s data according to which circle they belonged to (see the left part of Figure 8). For instance, P1’s 64 ratings on physical comfort were divided into five groups (circle A-E) and aver-

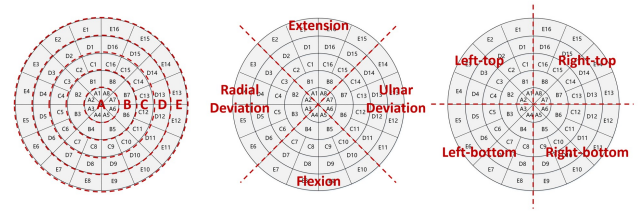


Figure 8: Three Different Ways of Grouping The 64 Regions for Analysis. Left) Regions were grouped based on the circle they belonging to. Middle) Regions were grouped based on the flexion/extension and radial/ulnar direction. Right) Regions were grouped based on the left/right and top/bottom position. The corresponding postures are shown in Figure 2.

aged each group into one mean rating scores, i.e., five scores for one participant. Taking the circle as the main factor, one-way ANOVAs showed significance (at $\alpha = 0.05$, the same below) on all three metrics ($F(\text{comfort})_{4,115} = 478.6$, $F(\text{time})_{4,115} = 686.7$, $F(\text{error})_{4,115} = 409.0$, all $p < 0.001$). Post-hoc pairwise Wilcoxon rank sum tests (for comfort score monotonically decreased on the sequence from circle A to E (all $p < 0.05$)). For time and error, post-hoc dependent t-test with Bonferroni adjustment showed that both monotonically increased (all $p < 0.05$).

Flexion > Extension ~ Radial Deviation > Ulnar Deviation

The performance of three metrics on the interface was obviously asymmetric, with ulnar generally better than radial and flexion better than extension (higher comfort ratings, shorter time as well as smaller error). Similar to the analysis of the circle effect, we grouped regions according to their positions (see the middle part of Figure 8). We merged 16 regions, including A2-3, B2-3, C3-6, D3-6 and E3-6, into the group *radial* (because of its relative position to the wrist, the same below. abbreviated as *r*). A4-5, B4-5, C7-10, D7-10 and E7-10 were grouped as *flexion* (*f*). The group *ulnar* (*u*) and *extension* (*e*) were merged by analogy. We first ran one-way ANOVAs on three metrics, taking the group as the factor. All of the results were significant ($F(\text{comfort})_{3,92} = 38.8$, $F(\text{time})_{3,92} = 32.4$, $F(\text{error})_{3,92} = 23.7$, all $p < 0.001$). Following the ANOVAs, we ran post-hoc pairwise Wilcoxon rank sum tests and dependent t-tests. For comfort score, $f > e \sim r > u$ (\sim represents insignificance, $V = 298, 143$ and 297.5 in sequence, $p = 0.00, 0.35, 0.00$). Time and error had the reverse order $f < e \sim r < u$ (For time, $t_{23} = -6.5, -1.1, -2.9$, $p = 0.00, 0.29, 0.01$. For error, $t_{23} = -6.4, -1.2, -2.8$, $p = 0.00, 0.22, 0.01$).

Left-bottom > Left-top > Right-bottom > Right-top

We also looked into the combination of the ulnar-radial-direction and extension-flexion, which also led into four groups, i.e., *left-bottom* (*lb*), *left-top* (*lt*), *right-bottom* (*rb*) and *right-top* (*rt*), as shown in the right part of Figure 8. We ran one-way ANOVAs on three metrics respectively with the location as the factor. The results indicated its significance ($F(\text{comfort})_{3,92} = 27.2$, $F(\text{time})_{3,92} = 22.4$, $F(\text{error})_{3,92} = 18.2$, all $p < 0.001$). Then, we ran post-hoc pairwise tests. For comfort score, the results showed the order

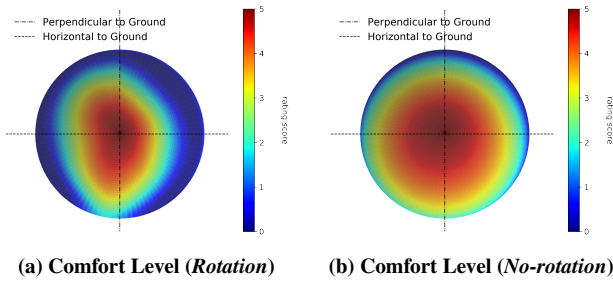


Figure 9: Smoothed Heat Map of Average Physical Comfort Score in Two Sessions. Bivariate spline approximation is employed for smoothing, with positive smoothing factor as 5.5 in both sessions.

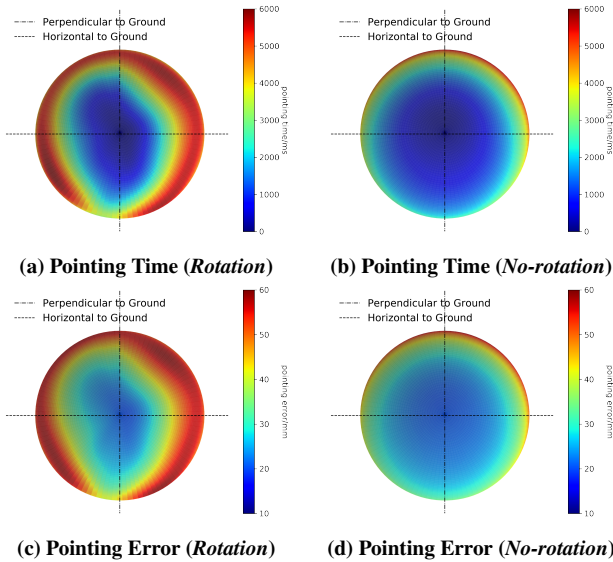


Figure 10: Smoothed Heat Map of Average Pointing Time And Error in Two Sessions. Bivariate spline approximation is used, with positive smoothing factor as 7e6 and 5e2 for time and error respectively. Two sessions share the same smoothing parameter.

$lb > lt > rb > rt$ ($V = 274, 276, 186.5$, all $p < 0.05$). The results of time and error hold the main order except that the difference between lb and lt is insignificant ($lb \sim lt < rb < rt$). For time, $t_{23} = -0.7, -9.1, -2.2, p = 0.49, 0.00, 0.04$. For error, $t_{23} = 0.5, -3.4, -7.9, p = 0.64, 0.00, 0.00$.

Protruding Area with Good Performance at Left-bottom Corner
From the heat maps we noticed two regions ($D8$ and $E8$) at the left-bottom corner having much better performance over other regions on the same circle, which resulted in protruding area on the heat maps of the *rotation* session. After averaging all participants' data on each single region respectively, we ran two Bonferroni outlier tests on three metrics on circle D and E separately. We detected the region $D8$ and $E8$ as the only outlier on their own circles with significantly greater comfort ratings, shorter time and lower error. On circle D , Bonferroni adjusted $p = 0.001, 0.003$ and 0.019 on physical comfort, time and error accordingly. On circle E , the three p -value are all smaller than 0.001 .

Significant Drop of The Performance from Radial to Ulnar Near The Flexion Maximum ROM

On circle C, D and E , the performance dropped significantly when the index finger changes the direction from radial to ulnar. This was reflected from the heat maps' slices at the vertical line. Based on each region's average data obtained in the last section, we further calculated the difference of each adjacent region-pair (i.e., first order difference) and ran Bonferroni Outlier tests on the difference sequence on circle C, D, E separately. Other than the significant outlier between $D8-D9$ and $E8-E9$ (both have $p < 0.01$ on all metrics), we found another outlier at $C1-C16$ ($p = 0.04, 0.03$ and 0.04 on the three metrics).

No-rotation Session

For the interface that was not rotating with the wrist, the heat maps were very different from the ones in the *rotation* session. We went through the identical analysis pipeline. We got the same results on the circle factor but different conclusions on both the " e, f, r, u " factor and " lb, lt, rb, rt " factor. Moreover, we did not find any irregular region.

Interior Circle Has a Better Performance Than Exterior Circle

After grouping the data into five circles, the one-way ANOVAs indicated significance on the circle effect ($F(\text{comfort})_{4,115} = 220.4$, $F(\text{time})_{4,115} = 175.1$, $F(\text{error})_{4,115} = 113.4$, all $p < 0.001$). Post-hoc analysis found the average physical comfort scores as a monotonically decreasing sequence from circle A to E , while both the average time and error are monotonically increasing sequences from A to E (all $p < 0.05$).

Flexion > Radial Deviation > Ulnar Deviation ~ Extension

We merged the data into the same four groups as the ones in the previous section, i.e., e, f, r and u . One-way ANOVAs on three metrics showed significance ($F(\text{comfort})_{3,92} = 28.0$, $F(\text{time})_{3,92} = 12.7$, $F(\text{error})_{3,92} = 10.2$, all $p < 0.001$). Post-hoc pairwise Wilcoxon rank sum test on the comfort ratings found the order $f > r > u \sim e$ ($V = 257.5, 273.5, 185.5, p = 0.00, 0.00, 0.16$ in sequence). While dependent t-test on the time and error found the order as $f < r < u \sim e$. For time, $t_{23} = -4.3, -2.3, -0.7, p = 0.00, 0.02, 0.23$. For error, $t_{23} = -3.5, -2.0, -1.7, p = 0.00, 0.02, 0.05$.

Left-bottom > Right-bottom > Left-top > Right-top

A different approach of grouping led into another four groups lb, lt, rb, rt (same as the previous section). One-way ANOVAs also presented significance on all three metrics ($F(\text{comfort})_{3,92} = 25.5$, $F(\text{time})_{3,92} = 14.7$, $F(\text{error})_{3,92} = 11.2$, all $p < 0.001$). A Wilcoxon rank sum test on the comfort scores showed the order as $lb > rb > lt > rt$ ($V = 244, 261.5, 232.5$, all $p < 0.05$). Dependent t-tests on the time and error found the corresponding reversed main order except the insignificant difference between the left-top and right-top parts, i.e., $lb < rb < lt \sim rt$. (for time, $t_{23} = -2.7, -3.6, -0.8, p = 0.01, 0.00, 0.22$, for error $t_{23} = -2.5, -3.3, 0.1, p = 0.01, 0.02, 0.54$).

Rotation Session VS. No-rotation Session

We first generally compared the two sessions by averaging all participants' data on all regions. The performance of the *no-rotation* session was better than the *rotation* session, with 41.2% higher average physical comfort score (3.18 ± 1.72 vs. 1.87 ± 2.08), 40.6% shorter average pointing time (1950.8 ± 1866.0 ms vs. 3283.0 ± 2089.8 ms) and 34.5% lower average error (26.7 ± 15.9 mm vs. 40.7 ± 18.8 mm).

The heat maps of the two sessions were very different. There were 17 out of 64 regions in the *rotation* session (see Figure 6a) that were not reachable by all 24 participants. In contrast, there was no unreachable region in the *no-rotation* session. We ran three two-way repeated measures ANOVAs on three metrics, taking the session (*rotation* vs. *no-rotation*) and the region as the main factors. The results were consistent with the general comparison and showed the significance of the main factors as well as their interaction (all $p < 0.05$). Participants were able to reach more regions on the interface, had much better performance, and gave much higher physical comfort ratings in the *no-rotation* session.

Most Regions in Two Sessions Had Significant Difference Except Circle A, E1 and E16

We investigated the difference between two sessions in detail by comparing every region's data respectively. Statistical tests revealed interesting results (Wilcoxon rank sum test for comfort score, dependent t-test for time and error): the difference mainly lay in circle *B-E* but not in circle *A*.

The performance of most regions in circle *A* (except *A3*) did not have significant difference between two sessions, with *A3* as the only region who had p -value smaller than 0.05 on pointing time and error ($t_{23} = 1.9$ and 3.3). For those regions in circle *B* to *E*, almost all regions' data were significantly different between the two sessions. Two interesting exceptional regions are *E1* and *E16*, where participants usually struggled to reach their wrist extension's limitation. Only one/three participants could reach *E1* in the *rotation/no-rotation* session, zero/two in the two sessions for *E16*. Hence they had similar bad performance and low comfort ratings, which indicated that the rotation of the forearm in the *no-rotation* session could not help participants at these extreme positions.

Landslide on Choosing The Preferred Session with 23 out of 24 liked No-rotation Session

When asked about the preference among the two sessions, 23 out of 24 participants chose the *no-rotation* session. We noted that although the feeling of being able to reach more regions might affect their choice, the participants' comments could provide solid reasons for their preference.

Nine participants mentioned the interface in the *no-rotation* session to be more "intuitive". "*The one that was not rotating with the hand felt more natural and intuitive.*" (P7) "*The second experiment [no-rotation] was easier because it adapted more in my logical expectation.*" (P15) Participants felt their movement was more limited in the *rotation* session. "*Comparing the previous session [no-rotation] it felt weird to see the surface rotating with my hand. My movement became limited.*" (P9) Some even found the rotation of the interface

to be annoying. "*The not rotating version made me feel much more comfortable. I can rotate my hand without any worries.*" (P10) "*I think the main reason [of choosing the no-rotation session] is that there is no need for me to worry about the [interface's] rotation any more. And my own rotation [of the forearm] can help me to reach more regions.*" (P3)

DISCUSSION

The Effects of Hand Range of Motion

The heat maps of the *rotation* session were barely affected by the rotation of the forearm, which reflected the effect of the hand anatomic structure on the index finger's movement.

Asymmetry

A number of participants were surprised when they found the range of motion of their hand was asymmetric. For instance, P6 said that she felt astonishing to find that her index finger can reach more on the left side (in the radial direction) than the right side, and more bottom part (in the flexion direction) than the top part. Specifically, we found that participants had better performance (shorter completion time and lower error) and gave higher comfort ratings with wrist flexion than extension. Radial deviation of the wrist was better than ulnar deviation on these three metrics. When dividing the regions into four groups according to the wrist torsion direction, we got the order of *flexion > extension ~ radial deviation > ulnar deviation* (the symbols ">" means better and "~" means similar, same below). Another way of grouping led into the order *left-bottom > left-top > right-bottom > right-top*. These findings could provide insights into understanding the effect of the human hand asymmetry on the index finger pointing operations.

Expansion From Wrist to Index Fingertip

We found that our results of the index finger's range of motion (ROM) were quite different from the findings on the wrist. Li et al. [23] drew out the convex hull of the wrist ROM. They found that users could reach further on extension than flexion and further on ulnar deviation than radial deviation. While in our study of the index finger movement, we found the reverse conclusion that users had a wider ROM in flexion than extension, as well as wider ROM in radial deviation than ulnar deviation. Our results are not in line with Carey et al. [4] who found users gave higher discomfort score in the flexion and radial deviation than extension and ulnar deviation. We found that users rated flexion and radial deviation more comfortable than extension and ulnar deviation. This might be explained by the role of the index finger, which could apply additional ROM of the fingertip on the wrist movement. This also indicated that previous findings on the wrist movement might need further studies to better understand hand-centric interface design.

Sharp Performance Drop on Right Side

We found two types of the performances significant drop on the heat maps of the *rotation* session. One appeared as the fingertip leaving the center of the interface. The comfort score decreased suddenly and the time and error increased substantially when the index finger was approaching its limitation (the yellow irregular circle in Figure 9a). This is in line with

the findings of Marler et al. [24]. The other appeared in the same circle at the vertical line (from C1 to C16, D8 to D9 and E8 to E9). It might be explained by the smaller finger movement range at the ulnar deviation than radial deviation, especially when participants' index finger was already close to the limitation on the flexion/extension direction (region C1 for extension and D8, E8 for flexion). This was also reflected from participants' comments. Four of them mentioned either right-top or right-bottom part to be very uncomfortable: "I must do my best to move the finger to the right top part. (P19).

The Effect of Fixing the Interface Rotation

In the *no-rotation* session, participants' rotation of the forearm could help them access more regions that were not reachable in the *rotation* session. The general comparison indicated that the average performance of the interface in the *no-rotation* session was much better than the one in the *rotation* session. The heat maps presented the results of the blended movement of the wrist and the forearm, which led to a much larger neutral area and different conclusions from the *rotation* session.

Preference for Interface Translation without Rotation

Some participants found the rotation of the interface to be annoying. "When I want to point at some position in the air, it is inevitable to slightly, even unconsciously rotate my wrist. But in this session [rotation] it would cause the interface to rotate. I did not expect this" (P4). P21 mentioned that he had to try very hard to keep the wrist static during the *rotation* session. "Because the interface's rotation was surprisingly nauseating!" (P21) In contrast, some participants liked the *no-rotation* session because it was more in line with their "logical thinking" (mentioned by P12, P20 and P23). "I like the not rotating one because I don't have to think much upon my behavior. But in the other session, I had to keep an eye on my wrist. It raised my body awareness... It was a bit distracting." (P13) Some participants pointed out the *absolute vs. relative* relationship between two sessions. For instance, P8 described the surface's rotation in the *rotation* session as more like a relative movement to the wrist and forearm, while the one in the *no-rotation* session was more like an absolute version. "I prefer the not rotating surface because there was no need for me to calculate the relative position." (P8)

Symmetry in Fixed Interface

Compared to the *rotation* session, the heat maps in the *no-rotation* session is more symmetric and regular. The difference between the interface's left and right half in the *no-rotation* session was much smaller than the one in the *rotation* session. This might be explained by the rotation of the forearm, which allowed participants to combine the flexion/extension with the radial/ulnar deviation and mitigate the left-right asymmetry of the wrist movement range. However, the bottom part was ranked higher than the top part, which again indicated that users were better at flexion than extension.

The order *flexion > extension ~ radial deviation > ulnar deviation* in the *rotation* sessions changed into *flexion > radial deviation > ulnar deviation ~ extension* in the *no-rotation*

session. The change of the extension's position in the order reflected the effect of the forearm rotation on the deviation. The order *left-bottom > left-top > right-bottom > right-top* in the *rotation* session showed that the "left>right" was the leading effect and the "top>bottom" was the secondary effect. While in the *no-rotation* session, the order turned into *left-bottom > right-bottom > left-top > right-top*. The leading effect became the "top>bottom" and the "left>right" became secondary. This was consistent with the change of the extension in the previous order.

New Ways of Pointing for Accessing Same Regions

During the *no-rotation* session, we observed some interesting postures among participants. They used different postures when trying to point at some regions that were beyond the extreme in the *rotation* session. Four examples that appeared most frequently were C12, D1, E4 and E12, as shown in Figure 11. When asked why they made such postures, many participants attributed it to the freedom of rotating their forearms. "It is intuitive. I don't have to worry about the wrist's rotation, so I can do anything." (P3) "When I figured out that I could rotate my wrist with the angle of the surface fixed [in the *no-rotation* session] I came up with many ideas to point at those balls." (P13)

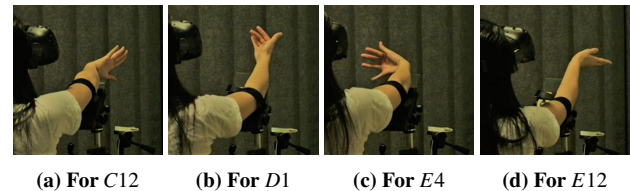


Figure 11: Four Interesting Postures in The *No-rotation* Session. 11 participants used the posture in (a) for regions around C12. 8 used the posture similar to (b) for regions around D1. 13 used (c)'s posture for regions around E4 and 6 used (d)'s posture for regions near E12.

Design Considerations for Hand-centric Interfaces

We propose the following strategies for designing hand-centric interfaces based on our experiment results.

No Rotation

According to the preference of the participants (23 out of 24 participants chose the *no-rotation* session), the design *interface not rotating with the wrist* is recommended, with a larger pointing area, higher comfort ratings, faster pointing speed, higher pointing accuracy. In practice, the interface's normal direction can be set in line with the axial direction of the forearm. The orientation of the interface could be determined by exterior measuring tools such as level meters.

Interface Around The Neutral Area

In line with the results of Marler et al. [24], we found significant performance decrease when participants reached out of their neutral area. We suggest designers position interface elements within the area where the color is red and orange on the heat map of the *no-rotation* session (comfort score above 3, see Figure 9b). This can help maintain a good user experience during the interaction.

Interaction in the Left-bottom

The heat maps in the *no-rotation* session are asymmetric, with the bottom half better than the top half, and left half moderately better than right half. We suggest designers shift the entire interface slightly to the left-bottom direction to the center of the irregular circle (see Figure 9b).

Use Flexion Movement

When designing the interaction with body-centric input surfaces, it's important to wrist the order of preferred movements obtained from the experiment of the *no-rotation* session, i.e., 1) *flexion* > *radial deviation* > *ulnar deviation* ~ *extension*, 2) *left-bottom* > *right-bottom* > *left-top* > *right-top*. The pair between the interface properties (e.g., function, frequency of use, etc.) and the preference order of the regions might provide helpful suggestions on their layout. For instance, the very frequently used “confirm button” could be placed at the center (left-bottom part, see Figure 9b) while the “cancel button” could be placed at the central symmetric position (right-top part).

LIMITATION AND FUTURE WORK

In this paper, we only discussed using the index finger of the right hand for interaction. We expect that the results of the left hand's index finger should be symmetric to right hand. Moreover, the interaction can involve not only just the index finger. The thumb and middle finger are two possible candidates in the future work.

To deal with the tradeoff between the tracking accuracy and the handsfree comfort during pointing, we chose the Leapmotion as the tracking system in our experiment. It had 4.43 mm tracking error and 32.9 ms latency on average compared to the Optitrack. Although the little tracking deviation and delay was not even noticed by most of the participants, it might imperceptibly influence the results. For instance, in the experiment, a user might touch a target sphere in VR while in the physical space she did not (a few millimeters away). We remind readers about the potential effects of using a low-cost hand tracking system.

We designed our hand-centric interface to use the wrist bones as the approximate center and the distance between index fingertip and the wrist center as the radius. There are a number of other body-centric designs that worth exploring. For instance, the finger-centric interface involves micro finger interaction. It can be centered at the metacarpophalangeal joint, and its radius can be set the same as each finger's length. Another example can be the elbow-centric interface that has the similar design but different center. We plan to further explore these designs in the future.

CONCLUSION

We have presented a qualitative exploration of the design space of body-centric interfaces attached to the wrist. We propose two rotation designs of the interface. One interface rotates with the user's wrist while the other interface's rotation is fixed. To compare the designs, we conducted a user study of a pointing task with 24 participants and measured the physical comfort, pointing time and pointing error of 64 regions on two interfaces to evaluate their usability. Our study

showed that participants preferred the one that not followed the wrist's rotation. We found interesting results when analyzing two interfaces individually, such as asymmetric performance on the interface, different preference order between two rotation designs, etc. We also proposed several tips for future designers on such a body-centric interface. Our prototype shows how such hands-free devices may allow for new kinds of interaction, and further exploration into new uses of information in mid-air.

REFERENCES

1. 2-16. eSkin Tattoo. <http://vivalnk.com/tattoo>. (2-16).
2. BI Intelligence Research Team. 2017. The Next Smartphone. www.read.bi/next-smartphone. (2017).
3. Gabor Blasko, Franz Coriand, and Steven Feiner. 2005. Exploring interaction with a simulated wrist-worn projection display. In *Proceedings of the IEEE Symposium on Wearable Computers*. 2–9.
4. Eilís Carey and Timothy Gallwey. 2005. Wrist discomfort levels for combined movements at constant force and repetition rate. *Ergonomics* 48, 2 (2005), 171–186.
5. Jessica R Cauchard, Mike Fraser, Teng Han, and Sriram Subramanian. 2012. Steerable projection: exploring alignment in interactive mobile displays. *Personal and Ubiquitous Computing* 16, 1 (2012), 27–37.
6. Edwin Chan, Teddy Seyed, Wolfgang Stuerzlinger, Xing-Dong Yang, and Frank Maurer. 2016. User elicitation on single-hand microgestures. In *Proceedings of the 2016 CHI Conference on Human Factors in Computing Systems*. ACM, 3403–3414.
7. Xiang'Anthony' Chen, Nicolai Marquardt, Anthony Tang, Sebastian Boring, and Saul Greenberg. 2012. Extending a mobile device's interaction space through body-centric interaction. In *Proceedings of the 14th international conference on Human-computer interaction with mobile devices and services*. ACM, 151–160.
8. Alexandru Dancu, Mickaël Fourgeaud, Mohammad Obaid, Morten Fjeld, and Niklas Elmqvist. 2015. Map Navigation Using a Wearable Mid-air Display. In *Proceedings of the 17th International Conference on Human-Computer Interaction with Mobile Devices and Services*. ACM, 71–76.
9. Barrett Ens, Ahmad Byagowi, Teng Han, Juan David Hincapié-Ramos, and Pourang Irani. 2016. Combining Ring Input with Hand Tracking for Precise, Natural Interaction with Spatial Analytic Interfaces. In *Proceedings of the 2016 Symposium on Spatial User Interaction*. ACM, 99–102.
10. Barrett M Ens, Rory Finnegan, and Pourang P Irani. 2014. The personal cockpit: a spatial interface for effective task switching on head-worn displays. In *Proceedings of the 32nd annual ACM conference on Human factors in computing systems*. ACM, 3171–3180.

11. G A Gescheider. 1988. Psychophysical Scaling. *Annual Review of Psychology* 39, 1 (1988), 169–200. DOI : <http://dx.doi.org/10.1146/annurev.ps.39.020188.001125> PMID: 3278675.
12. Jun Gong, Xing-Dong Yang, and Pourang Irani. 2016. WristWhirl: One-handed Continuous Smartwatch Input Using Wrist Gestures. In *Proceedings of the 29th Annual Symposium on User Interface Software and Technology (UIST '16)*. ACM, New York, NY, USA, 861–872. DOI : <http://dx.doi.org/10.1145/2984511.2984563>
13. Chris Harrison, Hrvoje Benko, and Andrew D Wilson. 2011. OmniTouch: wearable multitouch interaction everywhere. In *Proceedings of the 24th annual ACM symposium on User interface software and technology*. ACM, 441–450.
14. Chris Harrison, Shilpa Ramamurthy, and Scott E Hudson. 2012. On-body interaction: armed and dangerous. In *Proceedings of the Sixth International Conference on Tangible, Embedded and Embodied Interaction*. ACM, 69–76.
15. Chris Harrison, Desney Tan, and Dan Morris. 2010. Skinput: appropriating the body as an input surface. In *Proceedings of the SIGCHI Conference on Human Factors in Computing Systems*. ACM, 453–462.
16. Rayna Hollander. 2017. Apple just solved its biggest barrier to smartwatch adoption. www.newatlas.com/lg-watch-sport-review/48053/. (2017).
17. Takayuki Hoshi, Masafumi Takahashi, Kei Nakatsuma, and Hiroyuki Shinoda. 2009. Touchable holography. In *ACM SIGGRAPH 2009 Emerging Technologies*. 23.
18. Da-Yuan Huang, Liwei Chan, Shuo Yang, Fan Wang, Rong-Hao Liang, De-Nian Yang, Yi-Ping Hung, and Bing-Yu Chen. 2016. DigitSpace: Designing Thumb-to-Fingers Touch Interfaces for One-Handed and Eyes-Free Interactions. In *Proceedings of the 2016 CHI Conference on Human Factors in Computing Systems*. ACM, 1526–1537.
19. Hsin-Liu (Cindy) Kao, Christian Holz, Asta Roseway, Andres Calvo, and Chris Schmandt. 2016. DuoSkin: Rapidly Prototyping On-skin User Interfaces Using Skin-friendly Materials. In *Proceedings of the 2016 ACM International Symposium on Wearable Computers (ISWC '16)*. ACM, New York, NY, USA, 16–23. DOI : <http://dx.doi.org/10.1145/2971763.2971777>
20. Abid Ali Khan, Leonard O'Sullivan, and Timothy J Gallwey. 2009a. Effects of combined wrist deviation and forearm rotation on discomfort score. *Ergonomics* 52, 3 (2009), 345–361.
21. Abid Ali Khan, Leonard O'Sullivan, and Timothy J Gallwey. 2009b. Effects of combined wrist flexion/extension and forearm rotation and two levels of relative force on discomfort. *Ergonomics* 52, 10 (2009), 1265–1275.
22. Hugh Langley. 2017. Apple Watch Series 3 review. <http://read.bi/next-smartphone>. (2017).
23. Zong-Ming Li, Laurel Kuxhaus, Jesse A Fisk, and Thomas H Christophel. 2005. Coupling between wrist flexion–extension and radial–ulnar deviation. *Clinical biomechanics* 20, 2 (2005), 177–183.
24. R Timothy Marler, Salam Rahmatalla, Meagan Shanahan, and Karim Abdel-Malek. 2005. *A new discomfort function for optimization-based posture prediction*. Technical Report. SAE Technical Paper.
25. Denys JC Matthies, Simon T Perrault, Bodo Urban, and Shengdong Zhao. 2015. Botential: Localizing On-Body Gestures by Measuring Electrical Signatures on the Human Skin. In *Proceedings of the 17th International Conference on Human-Computer Interaction with Mobile Devices and Services*. ACM, 207–216.
26. Pranav Mistry and Pattie Maes. 2009. SixthSense: a wearable gestural interface. In *ACM SIGGRAPH ASIA 2009 Sketches*. ACM, 11.
27. Pranav Mistry, Pattie Maes, and Liyan Chang. 2009. WUW-wear Ur world: a wearable gestural interface. In *CHI'09 extended abstracts on Human factors in computing systems*. ACM, 4111–4116.
28. Florian Müller, Mohammadreza Khalilbeigi, Niloofar Dezfuli, Alireza Sahami Shirazi, Sebastian Günther, and Max Mühlhäuser. 2015. A Study on Proximity-based Hand Input for One-handed Mobile Interaction. In *Proceedings of the 3rd ACM Symposium on Spatial User Interaction*. ACM, 53–56.
29. Fred O'Connor. 2015. Study: HoloLens could replace PCs as the preferred workplace computer (Tractica). www.pcworld.com/article/2975103/study-hololens-could-replace-pcs.html. (2015).
30. Shuhei Ota, Yoshinari Takegawa, Tsutomu Terada, and Masahiko Tsukamoto. 2010. A method for wearable projector selection that considers the viewability of projected images. *Computers in Entertainment (CIE)* 8, 3 (2010), 17.
31. Mahfuz Rahman, Sean Gustafson, Pourang Irani, and Sriram Subramanian. 2009. Tilt Techniques: Investigating the Dexterity of Wrist-based Input. In *Proceedings of the SIGCHI Conference on Human Factors in Computing Systems (CHI '09)*. ACM, New York, NY, USA, 1943–1952. DOI : <http://dx.doi.org/10.1145/1518701.1518997>
32. Ismo Rakkolainen. 2007. How Feasible Are Star Wars Mid-Air Displays. In *Proceedings of the International Conference on Information Visualization*. 935–942.
33. Marcos Serrano, Anne Roudaut, and Pourang Irani. 2017. Visual Composition of Graphical Elements on Non-Rectangular Displays. In *Proceedings of the 2017 CHI Conference on Human Factors in Computing Systems (CHI '17)*. ACM, New York, NY, USA, 4405–4416. DOI : <http://dx.doi.org/10.1145/3025453.3025677>

34. Will Shanklin. 2017. LG Watch Sport review: The best standalone smartwatch. <http://www.businessinsider.com/apple-watch-series-3-smartwatch-adoption-2017-9>. (2017).
35. Ke Sun, Yuntao Wang, Chun Yu, Yukang Yan, Hongyi Wen, and Yuanchun Shi. 2017. Float: One-Handed and Touch-Free Target Selection on Smartwatches. In *Proceedings of the 2017 CHI Conference on Human Factors in Computing Systems (CHI '17)*. ACM, New York, NY, USA, 692–704. DOI : <http://dx.doi.org/10.1145/3025453.3026027>
36. Julie Wagner, Mathieu Nancel, Sean G Gustafson, Stephane Huot, and Wendy E Mackay. 2013. Body-centric design space for multi-surface interaction. In *Proceedings of the SIGCHI Conference on Human Factors in Computing Systems*. ACM, 1299–1308.
37. Martin Weigel, Sebastian Boring, Jürgen Steimle, Nicolai Marquardt, Saul Greenberg, and Anthony Tang. 2013. Projectorkit: easing rapid prototyping of interactive applications for mobile projectors. In *Proceedings of the 15th international conference on Human-computer interaction with mobile devices and services*. ACM, 247–250.
38. Martin Weigel, Vikram Mehta, and Jürgen Steimle. 2014. More than touch: understanding how people use skin as an input surface for mobile computing. In *Proceedings of the SIGCHI Conference on Human Factors in Computing Systems*. ACM, 179–188.
39. Karl DD Willis, Ivan Poupyrev, and Takaaki Shiratori. 2011. MotionBeam: a metaphor for character interaction with handheld projectors. In *Proceedings of the SIGCHI Conference on Human Factors in Computing Systems*. 1031–1040.
40. Christian Winkler, Julian Seifert, David Dobbstein, and Enrico Rukzio. 2014. Pervasive Information Through Constant Personal Projection: The Ambient Mobile Pervasive Display (AMP-D). In *Proceedings of the ACM Conference on Human Factors in Computing Systems*. 4117–4126.
41. Chao Xu, Parth H. Pathak, and Prasant Mohapatra. 2015. Finger-writing with Smartwatch: A Case for Finger and Hand Gesture Recognition Using Smartwatch. In *Proceedings of the 16th International Workshop on Mobile Computing Systems and Applications (HotMobile '15)*. ACM, New York, NY, USA, 9–14. DOI : <http://dx.doi.org/10.1145/2699343.2699350>
42. Goshiro Yamamoto and Kosuke Sato. 2007. PALMbit: A PALM Interface with Projector-Camera System. In *Adjunct Proceedings of Ubicomp*, Vol. 2007. 276–279.
43. Jingzhou Yang, R Timothy Marler, HyungJoo Kim, Jasbir Arora, and Karim Abdel-Malek. 2004. Multi-objective optimization for upper body posture prediction. In *10th AIAA/ISSMO multidisciplinary analysis and optimization conference*, Vol. 30.
44. Yang Zhang, Junhan Zhou, Gierad Laput, and Chris Harrison. 2016. SkinTrack: Using the Body as an Electrical Waveguide for Continuous Finger Tracking on the Skin. In *Proceedings of the 2016 CHI Conference on Human Factors in Computing Systems*. ACM, 1491–1503.